



Development of novel alginate based hydrogel films for wound healing applications

Rúben Pereira ^a, Anabela Carvalho ^b, Daniela C. Vaz ^c, M.H. Gil ^b, Ausenda Mendes ^a, Paulo Bártoolo ^{a,*}

^a Centre for Rapid and Sustainable Product Development, Polytechnic Institute of Leiria, Centro Empresarial da Marinha Grande, Marinha Grande, Portugal

^b Chemical Engineering Department, Faculty of Science and Technology of University of Coimbra, Pólo2, Coimbra, Portugal

^c Health Research Unit and School of Health Sciences, Polytechnic Institute of Leiria, Leiria, Portugal

ARTICLE INFO

Article history:

Received 25 May 2012

Received in revised form 21 August 2012

Accepted 30 September 2012

Available online 8 October 2012

Keywords:

Alginate

Aloe vera

Film

Hydrogel

Wound healing

ABSTRACT

Alginate and *Aloe vera* are natural materials widely investigated and used in the biomedical field. In this research work, thin hydrogel films composed by alginate and *Aloe vera* gel in different proportions (95:5, 85:15 and 75:25, v/v) were prepared and characterized. The films were evaluated regarding the light transmission behavior, contact angle measurements, and chemical, thermal and mechanical properties. These thin hydrogel films, prepared by crosslinking reaction using 5% calcium chloride solution, were also investigated relatively to their water solubility and swelling behavior. Results showed that *Aloe vera* improved the transparency of the films, as well their thermal stability. The developed films present adequate mechanical properties for skin applications, while the solubility studies demonstrated the insolubility of the films after 24 h of immersion in distilled water. The water absorption and swelling behavior of these films were greatly improved by the increase in *Aloe vera* proportion.

© 2012 Elsevier B.V. All rights reserved.

1. Introduction

Natural origin polymers such as alginate, collagen, DNA or RNA, are a class of materials widely used for biomedical applications [1,2]. These materials, obtained from nature, present a wide range of properties, namely biocompatibility, biodegradability and similarity with the human tissues. It is also possible to perform surface modifications in order to achieve a better cellular interaction [1]. According to their chemical structure, naturally derived polymers can be classified in three major classes: (1) polysaccharides, (2) proteins and (3) polyesters, being the first one of the most used in biomedical applications [2,3].

Hydrogels are tridimensional hydrophilic materials with the ability to absorb and retain large amounts of water when immersed in water or biological fluids, without dissolution [4,5]. They can be designed to be chemically stable over time, or to be degraded when in contact with the biological fluids by chemical (hydrolytic) and/or enzymatic degradation. Hydrogels based on natural polymers gained particular relevance on drug delivery [4] and wound healing [6] applications, due to their high water

content, biocompatibility, flexibility, porosity, smoothness and ability to incorporate and release therapeutic agents [1,5,7].

Alginate is an anionic polysaccharide, which is capable to form hydrogels under very mild conditions, at room temperature and in the absence of toxic solvents [2,8]. Alginate has been widely used and investigated due to its biocompatibility, biodegradability, relative low cost, low toxicity and gelling properties [1,8,9]. Commercial available alginates are typically extracted from brown algae (*Phaeophyceae*), including *Laminaria hyperborea*, *Laminaria digitata*, *Laminaria japonica*, *Ascophyllum nodosum*, and *Macrocystis pyrifera*. Alginates can also be obtained by bacterial biosynthesis from *Azotobacter* and *Pseudomonas*, exhibiting a more defined chemical structure and physical properties, when compared with the seaweed-derived alginates [8]. Its chemical structure contains blocks of (1,4)-linked β -D-mannuronate (M) and α -L-guluronate (G) residues (Fig. 1), that can be arranged in the form of homopolymeric sequences (MMM or GGG) or alternating sequences (MGMG) along the polymeric chain [10]. The content of M and G blocks, their distribution in the polymeric chain and the length of each block strongly determine the alginate physical and chemical properties and its gelling properties [10,11].

Alginate hydrogels are mostly prepared by external gelation, using calcium ions as cross-linking agents. The cation interacts and binds with guluronate blocks of alginate chains, forming the gel network [8,10]. Due to its high water content, elasticity, permeability and ability to create a moist environment in the wound bed, alginate gels have been widely used for the treatment of several

* Corresponding author at: Centre for Rapid and Sustainable Product Development, Polytechnic Institute of Leiria, Centro Empresarial da Marinha Grande, Marinha Grande, Portugal – Zona Industrial 2430-028 Marinha Grande, Portugal.

Tel.: +351 244569441; fax: +351 244569444.

E-mail address: paulo.bartolo@ipleiria.pt (P. Bártoolo).

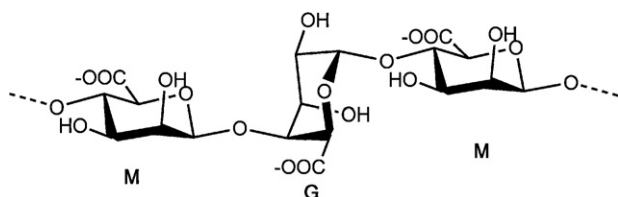


Fig. 1. Chemical structure of G-block and M-block in alginate.

kinds of wounds [12–16]. In particular, calcium alginate hydrogels were investigated and used for wound healing applications, due to both the hemostatic properties of the calcium ion and the ability of the gel to serve as a matrix for the aggregation of platelets and erythrocytes [7,8,17,18]. Additionally, the porosity of the hydrogels allows the entrapment/immobilization of therapeutic agents (drugs, growth factors, etc.), which are then released in the wound [8,10]. This approach can be used, for example, in the treatment of wound infections, which are frequently present in the early stages of the wound healing process.

The healing of a wound is a very complex and dynamic process that involves four main phases, which are distinct, sequential and overlapping [6]: hemostasis, inflammation, proliferation and tissue remodeling. A great variety of processes occur during these phases, including vasoconstriction, thrombogenesis, angiogenesis, synthesis of collagen, extracellular matrix (ECM) formation and ECM remodeling [6,18,19].

An ideal wound dressing should present adequate properties to create a favorable environment for the healing process, such as flexibility, durability, permeability to water vapor, adequate mechanical properties and adherence to the tissue. In addition, the dressing should have the ability to hydrate/dehydrate the wound, maintain a moist environment, protect the wound from infections and avoid maceration [6,12,17]. The incorporation of therapeutic agents into wound dressings and their topical release in the wound is an attractive approach to control the inflammatory reaction, prevent/eliminate infections and, simultaneously, to promote tissue regeneration. In the last years, topical administration of therapeutic agents into the wounds gained importance due to the limited efficacy of systemic treatment. This is related with the inadequate wound perfusion, which restricts the delivery of therapeutic agents to the wound [18,20]. Antibiotics, such as *gentamycin*, *ofloxacin* and *minocycline*, are commonly used in the treatment of wound infections, which are generally characterized by the presence of bacteria (e.g. *Staphylococcus aureus*, *Pseudomonas aeruginosa*) that can compromise the wound healing [1,17–20]. However, the constant administration of these drugs can increase the resistance of the microorganisms to them, which represents a great challenge for the scientific community [21]. An interesting solution to overcome this problem consists of the development of antimicrobial dressings based on natural materials with therapeutic properties, such as the *Aloe vera* plant [17,20].

Aloe vera (synonym *Aloe barbadensis* Miller) is a photosynthetic plant native from the South Africa, widely investigated for biomedical applications, and used in folk medicine for many years [22,23]. The fresh leaves of *Aloe vera* contain two main components: (1) a bitter yellow juice, commonly referred as “aloe juice” regulated by the U.S. Food and Drug Administration as a laxative and cathartic agent, and (2) a clear mucilaginous gel (*Aloe vera* gel) obtained from the leaf pulp, used in the topical treatment of skin wounds and burns [23]. According to Boudreau and Beland [23], the chemical composition of the *Aloe vera* gel can be divided in a liquid phase constituted by water (99–99.5%), and a solid phase (0.5–1.0%) containing soluble sugars (27.8%), lipids (5.9%), proteins (8.9%), non-starch polysaccharides and lignin (35%), vitamins (A, C, E) and minerals (e.g. calcium, potassium, sodium, magnesium).

Aloe vera gel is commonly used in various medical applications, essentially due to the biological activity of the polysaccharides and glycoproteins (e.g. lectins) present in the leaf pulp [24]. Polysaccharides are the most abundant and widely studied constituents of the *Aloe vera* gel consisting of linear chains of mannose and glucose [23], which represent more than 70% of the total sugars present in the plant [24]. Several polysaccharides were identified and isolated, including acemannan, pectic acid, galactan and glucomannan [24]. Acemannan, which chemical structure is illustrated at Fig. 2, is the main polysaccharide present in *Aloe vera*. It is a water soluble carbohydrate composed by glucose and mannose monomers linked by β -(1,4)-glycosidic bonds, which are susceptible to be degraded enzymatically [22,23]. It plays an important role in the wound healing process by inhibiting the bacterial growth and stimulating the macrophage activity [25].

Aloe vera gel has been attracting the interest of the scientific community due to its healing properties, anti-inflammatory, anti-septic and antimicrobial activity, which can be particularly important for wound healing applications [22,23]. The healing properties of *Aloe vera* are mainly attributed to the polysaccharides present in the plant, while the anti-septic and antimicrobial activity are related with the presence of antiseptic agents such as lupeol, salicyclic acid, urea nitrogen, cinnamic acid, phenols and sulfur, which have inhibitory activity against fungi, bacteria and viruses [22,23]. We hypothesized that *Aloe vera* can be an effective agent to promote the wound healing, and may be an alternative to the synthetic drugs, commonly used to eliminate bacterial infections in wounds.

For the best knowledge of the authors, this is the first report concerning the development of thin hydrogel films consisting of alginate and *Aloe vera* as a new system for wound healing and drug delivery applications. In our work, *Aloe vera*-Ca-alginate hydrogel films were prepared exploiting the hemostatic properties of calcium alginate gel and the therapeutic properties of *Aloe vera* compounds. On these films, alginate confers the adequate physical and mechanical properties, and allows the formation of a hydrogel using calcium as crosslink agent, due to its hemostatic properties (important for the hemostasis phase of wound healing). Moreover, alginate hydrogel also allows the incorporation of *Aloe vera* and/or other therapeutic agents, which are released into the wound during

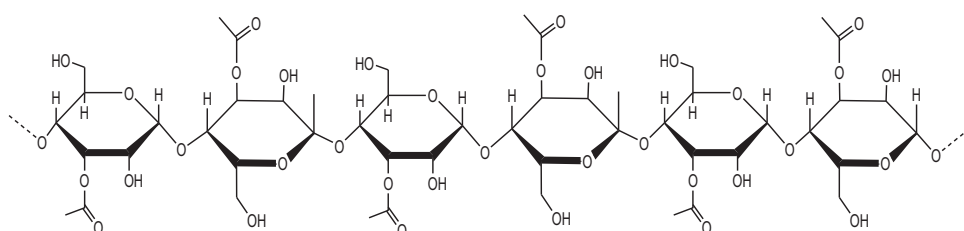


Fig. 2. Chemical structure of the polysaccharide acemannan present in *Aloe vera*.

the swelling to promote the healing process. Due to its properties, *Aloe vera* acts as an antimicrobial agent [21], eliminating possible infections (relevant in the inflammation phase of wound healing), and simultaneously stimulating the proliferation of fibroblasts and the synthesis of collagen [26,27], which are very important in the proliferation and remodeling phases of the wound healing. Additionally, it is expected that the incorporation of *Aloe vera* into the alginate films can contribute to preserve its therapeutic properties for a longer period of time, when compared with other formulations, such as creams.

In this work, we report the synthesis and characterization of alginate/*Aloe vera* films to be used as dressings for wound healing and drug delivery applications. The films were fabricated by solvent-casting process, and then submitted to a crosslinking step using calcium chloride as crosslinking agent, to obtain thin hydrogel films. The films were developed for application in soft tissues, in particular topical skin applications, and characterized through the evaluation of several properties, such as physical, thermal, chemical and mechanical properties. The swelling behavior and water solubility of the hydrogels were also investigated.

2. Experimental procedure

2.1. Materials

Sodium alginate was purchased from BDH Prolabo (VWR International, UK), and used as received. *Aloe vera*, ACTIValoe®, *Aloe vera* Gel Qmatrix 200X Flakes was kindly offered by Aloecorp (Broomfield, USA). Glycerol and calcium chloride (CaCl_2) were obtained from Scharlau (Spain) and Sigma/Aldrich Chemical Company (Portugal), respectively. Deuterium oxide (D_2O 99.9%) and 3-(trimethylsilyl)propionic acid-d₄ sodium salt (TSP-d4) were purchased from Sigma/Aldrich Chemical Company (Portugal). Ethylenediamine tetraacetic acid (EDTA) was purchased from V Reis (Portugal). Potassium bromide (KBr), for IR Spectroscopy was purchased from Fisher Chemical Company (Portugal).

2.2. Preparation of alginate-based films

Alginate and alginate/*Aloe vera* films were prepared using the solvent-casting process. Solutions of sodium alginate (1.5%, w/v) and *Aloe vera* (1.0%, w/v) were prepared by powder dissolution in distilled water, under mechanical agitation (alginate: 600 rpm; *Aloe vera*: 200 rpm), until complete dissolution. During the preparation of alginate solution, the plasticizer agent, glycerol, was added at a percentage of 15% (w/w), based on the weight of the alginate powder. Then, the solutions were transferred to an ultrasound system (15 min) and left to degasify for 12 h. Alginate neat films with glycerol (designated as AG) and without glycerol incorporation (designated as A) were prepared by casting 25 mL of solution into petri dishes ($\phi = 9.5$ cm). To prepare alginate/*Aloe vera* films, an appropriated volume of *Aloe vera* solution was slowly added to the alginate solution to obtain final alginate/*Aloe vera* proportions (v/v) of 95:5 (AGA5), 85:15 (AGA15) and 75:25 (AGA25). Afterwards, the mixture was stirred at 600 rpm for 30 min, and 25 mL of the mixture was casted into the petri dishes. The films were left to dry in room at 25 °C, with controlled humidity (50%) for two days, until completely dried.

To obtain thin hydrogels, dried film samples with appropriate dimensions were cut and immersed into a 5 mL of 5.0% (w/v) CaCl_2 aqueous solution, to allow the crosslinking for 5 min. Then, the hydrogels were washed with distilled water and dried at room temperature, until constant weight, before use.

2.3. Determination of the chemical composition of alginate by ¹H NMR spectroscopy

The chemical composition of alginate, the M/G ratio and the sequence of the blocks along the polymeric chain determine its functional properties, including the solubility, viscosity and gelification [28]. The chemical composition of alginate was assessed by ¹H nuclear magnetic resonance (NMR) spectroscopy. The ¹H NMR spectra of alginate in solution were recorded on a RMN Ultrashield Plus 400 spectrometer (Bruker, Germany), operating at 400 MHz for ¹H, under the following conditions: pulse angle of 90°, 512 scans, relaxation delay of 2 s, acquisition time of 4.096 s and a temperature of 80 °C. Prior to analysis, the molecular weight and the viscosity of the alginate were reduced by a mild partial acid hydrolysis, using 1 M HCl solution, according to the ASTM Standard F 2259 [29].

2.4. Film characterization

2.4.1. Film thickness

The film thickness was measured using a micrometer (Model 102-301, Mitutoyo) at nine different positions of the film with 0.001 mm of accuracy. The result was expressed as a mean of the measurements ± standard deviation (SD).

2.4.2. Film light transmission and transparency

Film light transmission and transparency were determined by spectrophotometry according to the method used by Norajit et al. [30]. Rectangular samples of the films (10 mm × 35 mm) were cut, placed into a spectrophotometer cell and their light barrier properties measured at wavelengths comprised between 200 and 800 nm, using air as a control. The transparency of the films was determined by Eq. (1) [30]:

$$\text{Transparency} = \frac{\text{Abs}_{600}}{x} \quad (1)$$

where Abs_{600} represents the value of absorbance at 600 nm, and x corresponds to the film thickness in millimeters. Three samples were used for each condition.

2.4.3. Determination of the calcium content

The concentration of calcium within the films after crosslinking was determined by atomic absorption spectroscopy (Spectrophotometer ICE 3000 Series, Thermo Scientific). Film samples with 2 cm of diameter were dissolved during 24 h in 10 mL of a calcium ion chelator, EDTA (0.05 M), to free the Ca^{2+} crosslinked ions within the alginate hydrogel, and then the solutions were analyzed. Calcium quantification was carried out in the absorption mode, using an air-acetylene flame at a wavelength of 422.7 nm [31]. Standard solutions of calcium with different concentrations were used to obtain the calibration curve, while the EDTA solution was used as a blank measurement. All tests were performed in triplicate.

2.4.4. Chemical characterization

The Infrared Spectroscopy technique was used to evaluate the chemical composition of the raw materials (alginate and *Aloe vera* in powder form), and to study the establishment of possible interactions between the compounds. The analysis were performed using an attenuated total reflectance (ATR) cell on the spectrophotometer FT/IR-4200 type A (JASCO, USA), in a range of 4000–500 cm^{-1} , at a 4 cm^{-1} resolution with 64 scans. The spectra of the raw materials were recorded in form of disc using a KBr matrix. Each test was repeated three times for each condition.

2.4.5. Thermal analyses

Thermal characterization was performed by differential scanning calorimetry (DSC) and thermogravimetric analysis (TGA), in

order to evaluate the influence of *Aloe vera* and the crosslinking process on the thermal properties of the films. Samples (3–4 mg) were heated in a STA 6000 – Simultaneous Thermal Analyzer (Perkin Elmer, USA) in a range of 30–350 °C at a constant heating rate of 10 °C/min, under a nitrogen atmosphere (20.0 mL/min). All the measurements were performed in triplicate.

2.4.6. Mechanical properties

The mechanical properties of the films were evaluated by tensile tests and compared with the skin values. The film tests were performed in several ways, namely in dry (crosslinked and non-crosslinked) and wet (crosslinked) states. Mechanical tensile tests were performed using an universal testing machine TCD-1000 (ChatillonTM) equipped with a 5 kN load cell. Film samples (15 mm × 50 mm) were tested at room temperature, using a gauge length of 20 mm and a crosshead speed of 15 mm/min. The mechanical properties of wet films were determined through the method of Sikareepaisan et al. [6]. The crosslinked specimens were immersed in distilled water for 30 s, and the excess of water removed with a filter paper. The specimens were then immediately tested. For each condition, five samples were tested. The results were evaluated in terms of tensile strength (TS) and elongation at break (E). Tensile strength was determined by the Eq. (2), while the elongation at break was calculated by Eq. (3):

$$TS = \frac{F_{\max}}{A} \quad (2)$$

$$E (\%) = \frac{L}{L_0} \times 100 \quad (3)$$

where F_{\max} corresponds to the maximum force at break, A represents the cross-sectional area of the specimen, L corresponds to the final length of the specimen at rupture, and L_0 represents the initial length of the specimen prior the test.

2.4.7. Surface film wettability

Wettability is an important parameter that affects several properties of the biomaterials, such as the water absorption, *in vitro* and *in vivo* degradation and cell interaction. The water contact angle was determined to evaluate the surface film's wettability, as well the influence of *Aloe vera* content in its properties. The static contact angle (θ) measurements were performed through the equipment OCA 20 (Data Physics) using water (10 μ l of volume drop and 2 μ l/s of velocity). For each condition, ten measurements were performed using the sessile drop method.

2.4.8. Water solubility and swelling behavior

It is widely recognized that water solubility and swelling are important properties for the characterization of biodegradable materials to be used in tissue regeneration and drug delivery applications. To determine the water solubility, crosslinked samples ($\phi = 2$ cm) of alginate/*Aloe vera* films were previously dried (at 37 °C for 24 h), and then immersed in 40 mL of distilled water at 37 °C and stirred at 120 rpm for 24 h. Afterwards, the samples were withdrawn from the medium, the excess of water removed with a filter paper and their wet weight immediately determined to calculate the water absorption. The samples were then dried in an oven, at 37 °C until constant weight, to determine the solubilized mass. Water absorption and water solubility were determined by Eqs. (4) and (5), respectively:

$$\text{Water absorption (\%)} = \left[\frac{W_w - W_d}{W_d} \right] \times 100 \quad (4)$$

$$\text{Water solubility (\%)} = \left[\frac{W_i - W_f}{W_i} \right] \times 100 \quad (5)$$

where W_w represents the wet weight of the films, W_d corresponds to the dry weight of the films, W_i represents the initial dry weight

of the film before immersion in distilled water, and W_f corresponds to the dry weight of the film after immersion.

The swelling behavior of the crosslinked film samples ($\phi = 2$ cm) was determined by immersion in acetate buffer (pH 5.5) to simulate the pH of the skin [32]. The samples were previously weighted (W_d) and immersed in 20 mL of solution at 37 °C. The films were removed from the solution at predetermined periods of time along 24 h, the excess of water withdrawn and its wet weight determined (W_w). To evaluate the influence of the pH in film swelling behavior, they were also immersed in two solutions, a 0.1 M HCl solution at pH 1.0 (simulated gastric fluid) and a simulated body fluid (SBF) at pH 7.4. The normalized swelling behavior was determined dividing the wet weight of the film after immersion by the initial dry weight before immersion using Eq. (6).

$$\text{Swelling} = \frac{W_w}{W_d} \quad (6)$$

To calculate the water solubility and swelling behavior, four samples were tested for each condition.

2.4.9. Statistical analysis

The data was presented as a mean of \pm SD for each result. The statistical analysis of the data was performed using the one-way analysis of variance (ANOVA) and the comparisons between two means through the Tukey's test. The statistical significance was considered for a $p < 0.05$. For each condition a minimum of three specimens were considered.

3. Results and discussion

3.1. Determination of the chemical composition of alginate by ¹H NMR spectroscopy

The chemical composition of the alginate can greatly influence its properties, which vary with the material batch, so it is fundamental to characterize the chemical structure of the alginate, to understand the behavior of this polysaccharide in the gelification process, the interaction with metals and salts, its solubility, the degradation behavior and kinetics release of drugs. For example, the gelation process of the alginates strongly affects their physical structure (strength and porosity) and depends on the affinity of certain ions with the G units, the M/G ratio and the number of repeated sequential G and M units [33–35]. The analysis of the chemical composition of the raw alginate powder used, allows to quantify the M/G ratio and the sequence of the blocks along the polymeric chain, which influence the properties of the resulting films.

Fig. 3 presents the ¹H NMR spectrum of the sodium alginate sample, which is similar to a spectrum of an alginate rich in M units [34]. The assigned signals in the spectrum correspond to the different protons of the sodium alginate structure, which nomenclature agrees with the ASTM Standard F 2259 [29]: alpha reducing ends (red-a); beta reducing ends (red-b); proton 1 from the guluronic unit (A); proton 5 from the GGM unit (B1) and MGM unit (B2); proton 1 from the MG unit (B3), MM unit (B4) and GG unit (C). It was possible to identify the characteristic signal of the guluronic acid anomeric proton (G-1) at 5.06 ppm, the guluronic acid H-5 (G-5) at 4.4 ppm, the mannuronic acid anomeric proton (M-1) and the C-5 of the alternating blocks (GM-5) overlapped at 4.7 ppm [35].

The chemical composition of the G and M units within the sodium alginate structure was determined through the signal intensity, reflecting the presence of the respective compounds. It is possible to observe that the alginate is rich in M units, representing about $54.09 \pm 1\%$ of the total alginate structure, while the M/G ratio is about 1.18. Regarding the chemical composition of the alginate, it is expected that the alginate hydrogels present a softer structure and lower porosity. The presence of a high number of M

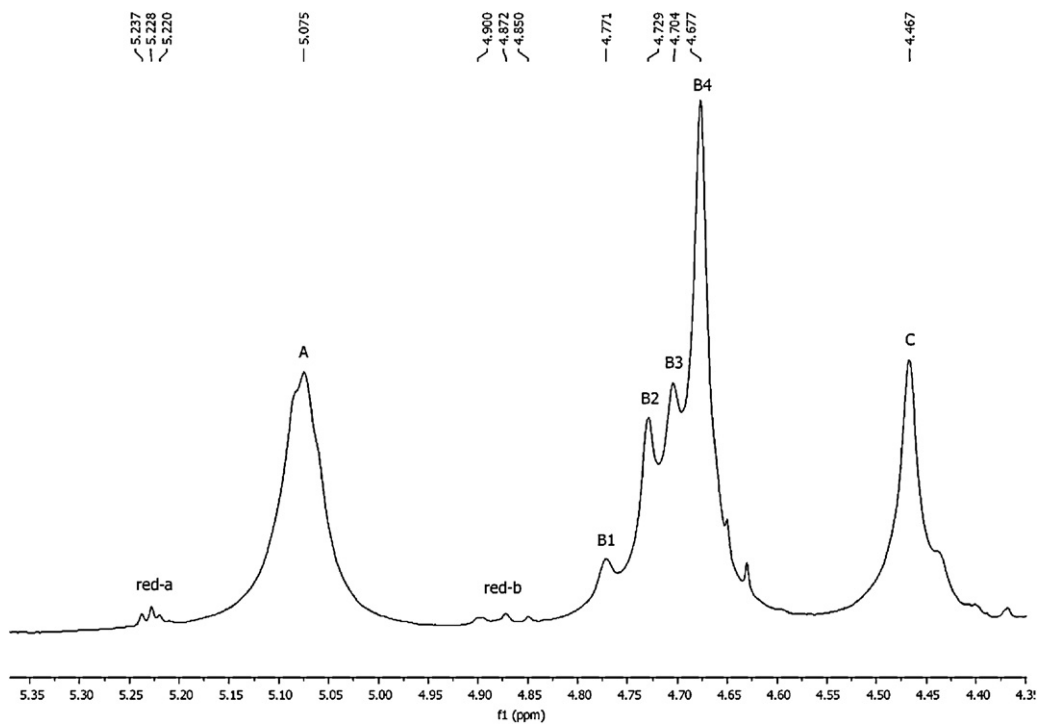


Fig. 3. ^1H NMR spectra of hydrolyzed alginate solution. The nomenclature of each peak is according the ASTM standard F 2259 [25].

units contributes to the decrease of the elastic segments into the alginate structure, which forms a more crosslinked structure [33]. In addition, the gels tend to present a high degree of swelling during the calcium cross-linking and subsequent shrinking, as well a lower stability along time [36]. These properties suggest that the resulting alginate film may present beneficial properties in terms of drug delivery and degradation kinetics.

3.2. Film characterization

3.2.1. Film thickness

Alginate/*Aloe vera* thin films were developed by the solvent-casting technique using a maximum *Aloe vera* incorporation of 25% and glycerol at 15%, based on optimization studies. These works comprised the evaluation of the following parameters: (i) alginate (0.75, 1.50 and 3.00%) and *Aloe vera* (0.75, 1.00 and 1.50%) concentration, (ii) plasticizer agent (glycerol) and its concentration (10, 15, 20 and 30%), (iii) proportion of alginate/*Aloe vera* (45/55–95/5), (iv) agitation velocity (100–800 rpm), (v) volume used to produce one film (20, 25 and 30 mL) and (vi) dry conditions (temperature and humidity). Findings were evaluated regarding the film homogeneity and thickness, mechanical properties, transparency and necessary time to dry. The glycerol was incorporated into the films to improve their flexibility and malleability, which are very important requisites for skin wound dressings.

The developed Alginate/*Aloe vera* films presented a smooth surface, high malleability and thicknesses comprised in a range 66.14–69.00 μm (Table 1). As illustrated in Table 1, the incorporation of *Aloe vera* within the alginate film caused a significant decrease ($p < 0.05$) in the film thickness, while the thickness of the prepared alginate/*Aloe vera* films was not significantly influenced ($p > 0.05$) by the proportion of *Aloe vera* (5%, 15%, 25%). Ma et al. [37] produced a bilayer structure of chitosan film and sponge as a scaffold for skin tissue engineering and a dermis substitute. Due to the slowly biodegradability of chitosan, it was considered that the dry thickness of chitosan sponge layers in a range 60–80 μm was adequate to allow the *in vitro* cell attachment and the *in*

vivo biodegradation. Considering the slow degradation of alginate *in vivo* conditions [10], the operating parameters were optimized to obtain films with adequate mechanical properties for skin application using the lower volume of alginate. Due to the lower content of polymer, it was obtained a thinner film than expected to facilitate the *in vivo* degradation of alginate and simultaneously satisfy the mechanical requisites for skin application. However, the film thickness is easily controlled by changing the volume of the solution deposited into the petri dishes.

3.2.2. Film light transmission and transparency

The light transmission and transparency are important properties in materials for wound healing applications [18]. Light transmission properties of the produced films are shown in Fig. 4. It is possible to observe that all the films present low light transmission in the ultraviolet (UV) light range, while in the visible range the light transmission significantly increases. In the case of

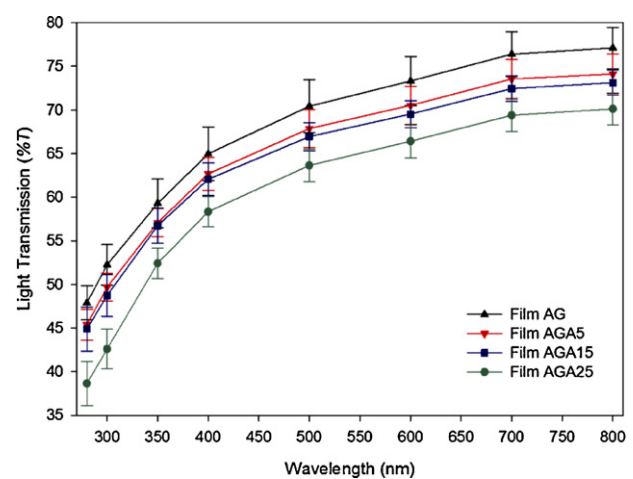


Fig. 4. Light transmission properties of the alginate/*Aloe vera* films.

Table 1Properties of the *Aloe vera* containing alginate hydrogels.

Film	Thickness (μm)	Transparency	Water solubility at 37 °C		Contact angle (°)		Calcium concentration (mg/L)
			Solubilized mass (%)	Water absorption after 24 h (%)	Rough side $^\psi$	Smooth side $^\psi$	
A	–	–	–	–	34.66 ± 1.23	35.11 ± 1.29	2.34 ± 0.52 ^a
AG	69.00 ± 0.79	1.28 ± 0.28	4.73 ± 0.65	157.38 ± 1.39	40.77 ± 1.20	42.24 ± 1.92	186.25 ± 1.21
AGA5	66.47 ± 1.77 [#]	1.60 ± 0.16	5.67 ± 1.13	159.13 ± 4.53	50.91 ± 1.54	52.52 ± 4.60	181.64 ± 2.98
AGA15	66.35 ± 1.90 [#]	1.90 ± 0.25	7.77 ± 0.53 [#]	163.69 ± 1.52	41.55 ± 1.02	39.28 ± 2.88	175.49 ± 6.59
AGA25	66.14 ± 2.25 [#]	2.11 ± 0.09 [#]	8.34 ± 0.45 [#]	183.72 ± 5.89 [#]	33.88 ± 1.86	30.25 ± 4.71	146.26 ± 6.39 [◊]

^a The calcium concentration within this film was determined without crosslinking step.^ψ All groups are statistically significant when compared between them ($p < 0.05$).[#] Statistically significant when compared with the control film AG ($p < 0.05$).[◊] Statistically significant when compared with the films AG, AGA5 and AGA15 ($p < 0.05$).**Fig. 5.** Influence of *Aloe vera* content in the transparency of the hydrogels immersed into SBF solution during 24 h.

the control film (AG), the film light transmission increased until a maximum of $76.09 \pm 2.24\%$, due to the increase in the wavelength. The incorporation of *Aloe vera* within the alginate films caused a decrease ($p < 0.05$) in the light transmission, due to the high retention of the light, reaching maximum values of light transmission of $73.26 \pm 4.76\%$ (Film AGA5), $72.07 \pm 1.69\%$ (Film AGA15) and $69.32 \pm 1.79\%$ (Film AGA25). In the UV light range, specifically at 200 nm, very low values of light transmission are observed ranging between 0.05% and 0.06%, which agrees with the results for alginate neat films reported by Norajit et al. [30]. The low values of light transmission in the UV light range can be beneficial for the proposed applications, protecting the wound from UV light. On the other hand, the high light transmission in the visible light can be an advantage for skin applications, allowing the monitoring of the healing process without removing the film.

Regarding the influence of *Aloe vera* in the film transparency, results presented in Table 1, show that the increase in the *Aloe vera* proportion raises the film transparency. It is also possible to observe (Fig. 5) that the crosslinked thin hydrogel films with high proportions of *Aloe vera* exhibit high transparency in a wet state, after immersion in SBF. These results show the positive influence of the *Aloe vera* in the light transmission and transparency film properties.

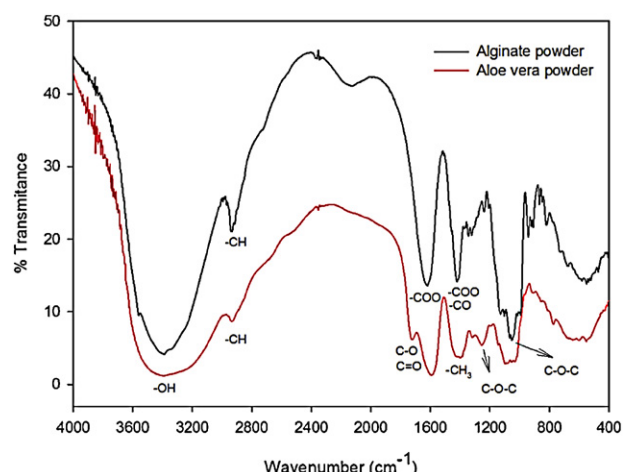
3.2.3. Chemical characterization

The evaluation of the chemical composition of the alginate films is very important to recognize the chemical groups present in their chemical structure, as well to investigate the possible establishment of chemical interactions between the compounds. In Fig. 6, it is possible to observe the FTIR spectrum of the non-processed sodium alginate and *Aloe vera*.

Pure alginate presents two characteristic absorption bands around 1620 cm^{-1} and 1421 cm^{-1} , corresponding to the asymmetric and symmetric stretching vibration of the COO groups, respectively. The –CH vibration band occurs at 2935 cm^{-1} and 1420 cm^{-1} , which can be overlapped with the COO vibration bands. The band from the C–O–C stretching occurs around 1051 cm^{-1} and a large absorption band at 3388 cm^{-1} , due to the stretching vibration of OH group [9,38,39].

Aloe vera presents characteristic absorption bands at 3390 cm^{-1} and 2931 cm^{-1} , which can be attributed to the –OH group and –CH vibration, respectively. At 1719 cm^{-1} it is also possible to observe a weak absorption band, probably related to the C–O and C=O linkages, from the aldehyde/ketone and carboxylic acid groups. Furthermore, at 1407 cm^{-1} and 1254 cm^{-1} were also detected absorption bands, probably due to the presence of CH_3 vibration and C–O–C groups, respectively [40,41].

Fig. 7 presents the most important vibration modes from the functional groups in the prepared films. It seems that there are no significant differences between the pure alginate film (AG) and the alginate films containing *Aloe vera* (AGA5, AGA15, AGA25). In all spectra's, it is possible to identify the vibration bands from the COO, CH, C–O, OH and C–O–C groups. The bands corresponding to the COO and C–O linkages tend to be more intense ($1290\text{--}1600\text{ cm}^{-1}$) with the increase of alginate content in the film and consequent decrease of the *Aloe vera* content. This behavior can also be

**Fig. 6.** Overlap of the FTIR spectra, recorded in transmittance mode, from the alginate and *Aloe vera* raw-materials.

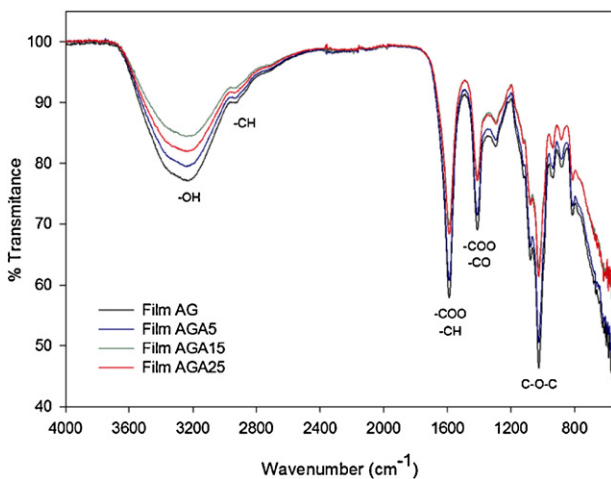


Fig. 7. Overlap FTIR spectra of the several crosslinked alginate-based films.

dependent on the interaction degree between the COO^- groups and the Ca^{2+} ions, due to the crosslinking reaction with the CaCl_2 occurring in these sites [31]. These results agree with the values obtained from the calcium content determination, which indicate a decrease in the calcium concentration within the film with the decrease in the alginate content (Table 1).

3.2.4. Thermal analysis

The DSC analysis, performed with the unprocessed alginate, indicates the existence of two endothermic peaks and one exothermic one (Supplementary Fig. S1). The first endothermic peak (69.53°C) is attributed to the water loss of hydrophilic polymer groups, while the second one (187.56°C) corresponds to the alginate melting temperature [9,42,43]. The exothermic peak appearing at 242.93°C is attributed to the polymer degradation [9,43], as can be confirmed by the TGA analysis (Supplementary Fig. S1).

The DSC analysis, performed with the unprocessed *Aloe vera*, shows the continuous degradation in the temperature range (30 – 350°C). The DSC curve present various exothermic peaks, while the TGA curve is characterized by continuous and overlapping stages of degradation (Supplementary Fig. S2).

The DSC curves of the produced films are illustrated in the Fig. 8. The DSC curve of the alginate film without glycerol (Film A) is characterized by one endothermic peak (57.32 ± 5.11), probably due to

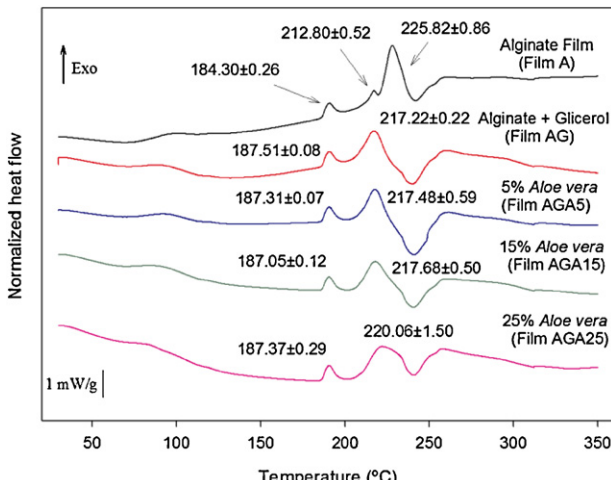


Fig. 8. DSC thermograms of the alginate and alginate/*Aloe vera* films.

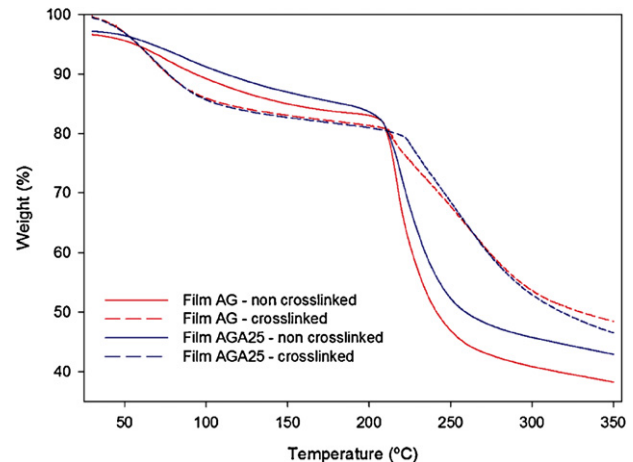


Fig. 9. TGA thermograms of the films AG and AGA25: influence of *Aloe vera* content and crosslinking process on the films weight loss profile.

the water loss [43], and three exothermic peaks. The exothermic peak appearing at 184.30°C can be attributed to a recrystallization phenomenon [43], while the peaks at 212.80°C and 225.82°C correspond to the film degradation. The TGA analysis demonstrates a great slope in the weight loss curve of the film at around 212°C , which continues until approximately 250°C , and can be attributed to the alginate degradation. The conversion of alginate powder within the films caused a decrease in the degradation temperature, which may be a result of the reduced strength of polymer-polymer interaction, and the plasticizer effect of the water during the film formation. It is possible to observe the appearance of an exothermic peak at 217.22°C (Fig. 8) for the alginate films with incorporation of glycerol. This peak presents an intermediate value between the two exothermic peaks (212.80°C and 225.82°C) observed in the alginate film, and may be a result of their blending. An increase in the recrystallization temperature can also be due to the establishment of hydrogen bonds between both the hydroxyl groups of the glycerol and the carboxyl/hydroxyl groups of alginate.

The incorporation of different proportions of *Aloe vera* does not cause significant alterations in the DSC curves of the films (Fig. 8). However, it is possible to observe a slight increase in the degradation temperature (217.22 – 220.06°C) of the films, as a consequence of the increase in *Aloe vera* proportion. The thermogram of the alginate film with 25% of *Aloe vera* (AGA25) presents a broad decomposition peak, when compared with the other films. These results suggest an increase in the thermal stability of the films, which can be attributed to the chemical interactions between the alginate and *Aloe vera*.

The weight loss profiles of the alginate neat film (Film AG) and alginate film with 25% of *Aloe vera* (Film AGA25), before and after the crosslinking process is presented in Fig. 9. It is possible to observe that all films show two well-defined stages of weight loss. The first one is a slow weight loss stage occurring between 70 – 150°C for the non-crosslinked films, and 40 – 100°C in the case of crosslinked films, as a consequence of the film dehydration with the loss of water [42,43]. The crosslinked films present higher weight loss percentage in the first stage of degradation, probably due to the immersion in an aqueous solution of CaCl_2 to allow the crosslinking. The second stage of degradation occurs in the range 200 – 280°C for the non-crosslinked films, and 205 – 325°C in the case of crosslinked films attributed to the film degradation [42,43]. Crosslinking process seems to increase the thermal stability of the films by increasing the degradation temperature of both AG (201.05 – 209.10°C) and AGA25 (201.69 – 220.20°C) films. The crosslinking process also decreases the films weight loss at 350°C .

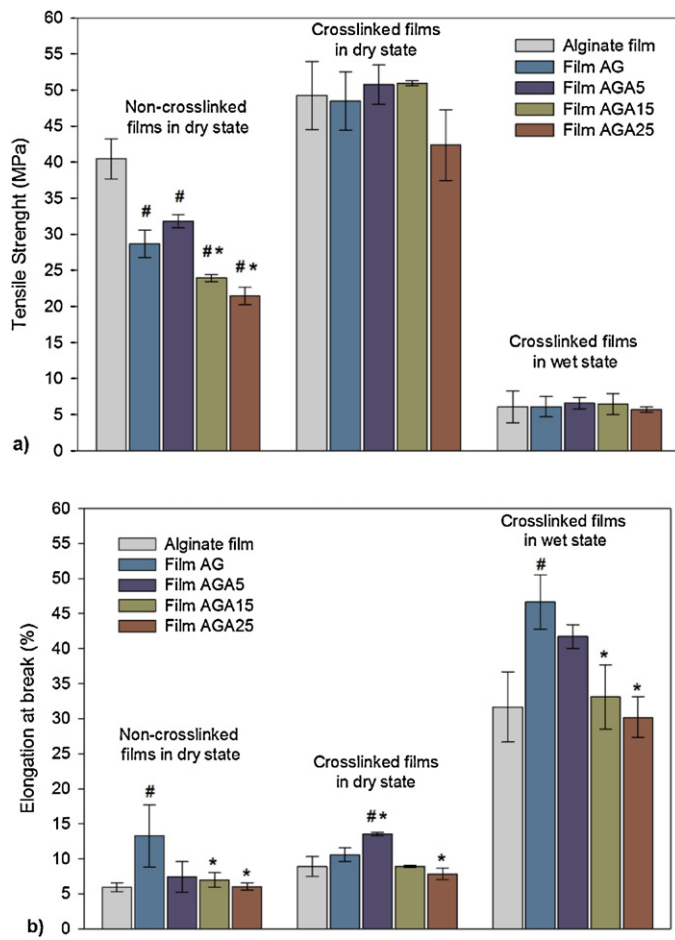


Fig. 10. Mechanical properties of the films: Tensile strength (a) and elongation at break (b). #Statistically significant when compared with film A ($p < 0.05$); *statistically significant when compared with film AG ($p < 0.05$).

The weight loss of the non-crosslinked AG film was 61.79% while the value was 52.72% for the crosslinked film. In the case of AGA25 film, the weight loss in the non-crosslinked state was 57.07%, while in the crosslinked state the value was slightly lower (53.48%). The TGA analysis seems to demonstrate that *Aloe vera* can contribute to increase the thermal stability of the films.

3.2.5. Mechanical characterization

An ideal wound dressing should present good mechanical properties and maintain their integrity during use [12]. Additionally, the films should present adequate resistance to the mechanical abrasion and be flexible to follow the skin movements. The mechanical properties of the films were evaluated regarding its tensile strength and elongation at break for different possibilities of use as shown in Fig. 10. The properties of the alginate neat film without incorporation of the plasticizer glycerol (Film A) were also investigated.

Dry films in non-crosslinked state exhibit values of tensile strength and elongation at break in a range of 21.44–40.44 MPa and 5.94–13.27%, respectively. The inclusion of glycerol within the alginate film has a significant influence in its mechanical properties ($p < 0.05$), causing a significant reduction in the rigidity, by decreasing the tensile strength (40.44–28.66 MPa) and increasing the elongation at break (5.94–13.27%). This behavior can be explained by the plasticizing effect of the glycerol, which improves the free volume between the polymeric chains, reducing the polymer-polymer interactions and increasing the mobility of the polymeric chains [44]. The addition of *Aloe vera* was responsible for a slight decrease in the tensile strength and elongation at break of the films,

which can be explained by the reduction on the alginate and glycerol content within the films.

After the crosslinking, all films present an increase in their tensile strength, when compared with the non-crosslinked films, exhibiting values in the range of 42.36–50.91 MPa. Similar observations on the effect of the crosslinking process were stated by Sikareepaisan et al. [6]. Regarding the elongation at break, the values are in a range of 7.86–13.56%, which are very similar to the values of the non-crosslinked films. No significant influence ($p > 0.05$) in the tensile strength of the films was observed with a variation of the *Aloe vera* proportion.

The crosslinked films present higher malleability and a very smooth surface when immersed in distilled water for 30 s. It was observed a great decrease in the film tensile strength, which varies between 5.70 MPa and 6.58 MPa, while the elongation at break suffered a significant increase (30.19–46.66%), when compared with the non-hydrated films in the crosslinked state (7.86–13.56%). These results are correlated with the plasticizing effect of the absorbed water molecules during the immersion [6]. The addition of *Aloe vera* has no significant influence ($p > 0.05$) in the tensile strength of the wet films, as shown in Fig. 10a, contributing to a decrease in the elongation at break, due to the decrease in the glycerol content within the films.

The values of the tensile strength of the skin are usually in the range 2.5–16 MPa [12], and the elongation is approximately 70% in the most flexible zones [45]. Comparing these values with the mechanical properties of the developed films, all films present adequate properties for skin application. However, the elongation of the non-hydrated films is quite far from the average skin value, which suggests that it is preferable to use them in less flexible zones of the body.

3.2.6. Surface film wettability

Table 1 presents the contact angle of the prepared films in both rough and smooth sides. For the same film, the results revealed no significant changes in the contact angle value. The addition of 15% of glycerol (Film AG) increased the contact angle of the film, comparatively to the pure alginate film (Film A), which can be attributed to the diffusion of glycerol from the film to the droplet, changing the surface properties. The obtained contact angle values are comprised between 33.88° and 50.91°, highlighting the hydrophilic properties of the films. The lower value was observed for the film with higher *Aloe vera* content (AGA25), which can be related with the high affinity of the *Aloe vera* with the water [41].

3.2.7. Water solubility and swelling behavior

The water solubility and swelling behavior of hydrogels were investigated at physiological temperature (37 °C), to evaluate their potential to be used in applications requiring a permanent contact with water or biological fluids, such as blood and wound exudate.

The water solubility of the films is comprised between 4.73% and 8.34%, as indicated in the Table 1. The results indicate that the films are practically insoluble after immersion in distilled water for 24 h, once the weight change before and after the immersion is not statistically different ($p > 0.05$). However, the solubilized mass of the films increased ($p < 0.05$) with the increase in *Aloe vera* proportion, which may be due to the higher water absorption (Table 1).

The influence of *Aloe vera* on the water absorption and swelling behavior of the films was investigated using acetate buffer pH 5.5 as a skin model. Results show that an increase in the *Aloe vera* proportion within the films contributes to improve the water absorption capacity, as it is possible to observe in Fig. 11a. More specifically, it was found that the incorporation of 5% of *Aloe vera* does not have a significant influence in the water absorption ($p > 0.05$), while the incorporation of 15% and 25% contributes to a significant increase in this parameter ($p < 0.05$). The swelling behavior of the

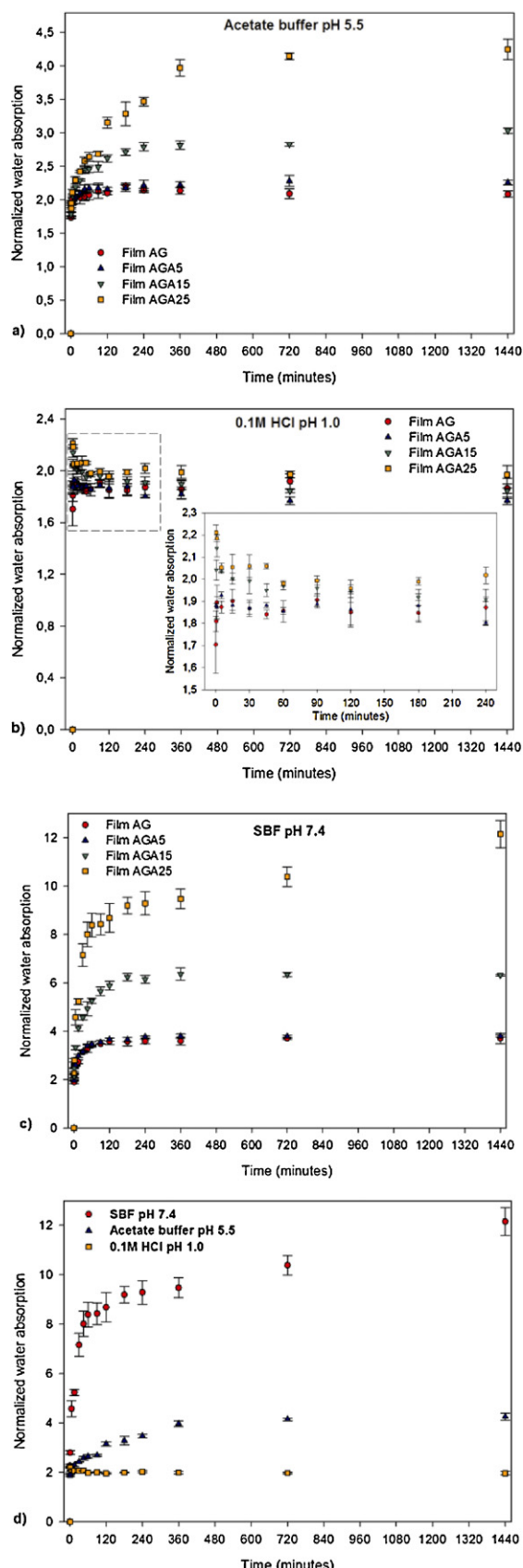


Fig. 11. Swelling behavior of the films immersed in acetate buffer pH 5.5 (a), 0.1 M HCl pH 1.0 (b), and simulated body fluid pH 7.4 (c). Swelling behavior of the film AGA25 immersed in solutions with different pH (d).

hydrogels is also dependent of the *Aloe vera*, being possible to observe an increase in the time required to reach the equilibrium as a function of the increase on the *Aloe vera* content: 120 min, 240 min and 720 min, for the films AG/AGA5, AGA15 and AGA25, respectively.

To investigate the influence of the pH solution on the water absorption and swelling behavior, the films were also immersed in 0.1 M HCl (pH 1.0) and SBF (pH 7.4). The films immersed in HCl (Fig. 11b) presented the lowest water absorption due to the protonation of the carboxylic groups. The pH of HCl solution is below the pK_a of the ionizable groups of the alginate ($M = 3.38$ and $G = 3.65$ [46]), resulting in a low swelling behavior [47]. In addition, the glycosidic linkages of alginate are susceptible to be cleaved in acid medium, resulting in acid hydrolysis and consequently in the film degradation [48]. Therefore, the films presented an instantaneous absorption of water (Fig. 11b) followed by a progressive release of the absorbed water until reaching the equilibrium. Contrary, the films immersed in SBF exhibited the higher water absorption, as it is possible to observe in Fig. 11c. In this solution, the carboxylic groups of the alginate remain in the ionizable form (COO^-) increasing the electrostatic repulsion between them and improving the swelling of the hydrogel. The films immersed in SBF swelled more extensively and more slowly, requiring more time to reach the equilibrium. Fig. 11d clearly shows the influence of pH on the water absorption and swelling behavior of the film AGA25 during 24 h of immersion. The data revealed that the water absorption for SBF was 6 times greater than 0.1 M HCl and 3 times greater than acetate buffer.

During the swelling of the hydrogel, it is expected that some *Aloe vera* compounds diffuse from the hydrogel to the wound bed due to the penetration of water, resulting in the topical release. The release of the *Aloe vera* compounds directly into the wound bed will increase the effectiveness of their action, when compared with other methods of administration (e.g. oral, systemic), which could be very important for the wound healing process. According to the results, it is also expected that the release rate of the compounds could be controlled through the composition of the hydrogels, once this parameter has great influence in the water absorption.

The extent of crosslink may be an additional factor explaining the differences observed in the water absorption ratio of the films. To evaluate the extent of crosslink, the calcium content within the films after crosslinking was determined by atomic absorption spectrophotometry (Table 1). The analysis performed to the non-crosslinked alginate neat film (Film A) revealed the presence of a residual content in Ca^{2+} ($2.34 \pm 0.52 \text{ mg/L}$), while the crosslinked AG film showed a concentration of about $186.25 \pm 1.21 \text{ mg/L}$, confirming the crosslinking process. In the case of the films containing *Aloe vera*, the analysis indicates a progressive decrease in the calcium content, as the *Aloe vera* proportion increases ($p < 0.05$). This result is attributed to the decrease in the content of alginate within the films as well as to the fact that the *Aloe vera* is not crosslinked with calcium. According to these results, the films with high proportions of *Aloe vera* present low extent of crosslink, which can lead to a reduced retractive force between the polymeric chains and allow the absorption of larger amounts of water.

4. Conclusions

In this work, a simple and rapid methodology was proposed to prepare novel alginate/*Aloe vera* thin films by solvent-casting process. The analyzed thin films present dry thicknesses comprised in the interval between 66.14 and 69.00 μm , as well as homogenous surface and high malleability. Light transmission and transparency studies showed the positive influence of the *Aloe vera* on these properties. The proposed films seem to be a good barrier for the

transmittance of UV light, protecting the wound. The crosslinking reaction using 5% CaCl₂ resulted in the increase of film's transparency, mechanical strength and water absorption properties. The chemical analysis allows concluding that the *Aloe vera* and alginate are compatible materials, with high similarity in terms of the main chemical groups. The alginate/*Aloe vera* films obtained do not present phase separation or incompatible domains. Due to the high complexity of the *Aloe vera* chemical structure, it was not possible to confirm all the interactions between the materials. The incorporation of *Aloe vera* does not change significantly the chemical properties of the films, while contributing to increase their thermal stability by increasing the degradation temperature and decreasing the film's weight loss. The crosslinked films are practically insoluble after immersion in distilled water for 24 h, presenting adequate mechanical properties for skin application. The water uptake and swelling behavior of the prepared films are dependent on both *Aloe vera* proportion within the film and the pH of solution. The increase in *Aloe vera* content caused a significant increase in the water absorption, probably due to the hydrophilic properties of the *Aloe vera*, and the extension of the crosslink. Contact angle results demonstrate the hydrophilic properties of the films, which agrees with the water uptake results. This research work also suggests that alginate/*Aloe vera* films have suitable properties for wound healing and drug delivery applications.

Acknowledgments

The authors would like to thank ZeusQuímica Lda and Aloecorp Inc. for kindly supplying the *Aloe vera* used for this research work. We are also grateful to Dr. Pedro Cruz for his support in ¹H RMN analysis and Ms. Célia Gomes for her support in the atomic absorption spectroscopy experiments. The authors Rúben Pereira, Ausenda Mendes and Paulo Bártoolo would like to thank the support of the Portuguese Foundation for Science and Technology through the strategic project Pest-OE/EME/UI4044/2011.

Appendix A. Supplementary data

Supplementary data associated with this article can be found, in the online version, at <http://dx.doi.org/10.1016/j.ijbiomac.2012.09.031>.

References

- [1] S. Huang, X. Fu, *Journal of Controlled Release* 142 (2010) 149–159.
- [2] D. Puppi, F. Chiellini, A.M. Piras, E. Chiellini, *Progress in Polymer Science* 35 (2010) 403–440.
- [3] Z. Liu, Y. Jiao, Y. Wang, C. Zhou, Z. Zhang, *Advanced Drug Delivery Reviews* 60 (2008) 1650–1662.
- [4] J.F. Almeida, P. Ferreira, A. Lopes, M.H. Gil, *International Journal of Biological Macromolecules* 49 (2011) 948–954.
- [5] J. Jagur-Grodzinski, *Polymers for Advanced Technologies* 21 (2010) 27–47.
- [6] P. Sikareepaisan, U. Ruktanonchai, P. Supaphol, *Carbohydrate Polymers* 83 (2011) 1457–1469.
- [7] P. Laurienzo, *Marine Drugs* 8 (2010) 2435–2465.
- [8] K.Y. Lee, D.J. Mooney, *Progress in Polymer Science* 37 (2012) 106–126.
- [9] R. Pereira, A. Tojeira, D.C. Vaz, A. Mendes, P. Bártoolo, *Preparation, International Journal of Polymer Analysis and Characterization* 16 (2011) 449–464.
- [10] A.D. Augst, H.J. Kong, D.J. Mooney, *Macromolecular Bioscience* 7 (2006) 623–633.
- [11] R.A. Rezende, P.J. Bártoolo, A. Mendes, R.M. Filho, *Journal of Applied Polymer Science* 113 (2009) 3866–3871.
- [12] L. Wang, E. Khor, A. Wee, L.Y. Lim, *Journal of Biomedical Materials Research* 63 (2002) 610–618.
- [13] Y. Suzuki, M. Tanihara, Y. Nishimura, K. Suzuki, Y. Yamawaki, H. Kudo, Y. Kakinami, Y. Shimizu, *Journal of Biomedical Materials Research* 48 (1999) 522–527.
- [14] C.-T. Chiu, J.-S. Lee, C.-S. Chu, Y.-P. Chang, Y.-J. Wang, *Journal of Materials Science Materials in Medicine* 19 (2008) 2503–2513.
- [15] K.T. Shalumon, K.H. Anulekha, S.V. Nair, S.V. Nair, K.P. Chennazhi, R. Jayakumar, *International Journal of Biological Macromolecules* 49 (2011) 247–254.
- [16] H.-E. Thu, M.H. Zulfakar, S.-F. Ng, *International Journal of Pharmaceutics* 434 (2012) 375–383.
- [17] T. Abdelrahman, H. Newton, *Surgery* 29 (2011) 491–495.
- [18] J.S. Boateng, K.H. Matthews, H.N.E. Stevens, G.M. Eccleston, *Journal of Pharmaceutical Sciences* 97 (2008) 2892–2923.
- [19] S. Guo, L.A. DiPietro, *Journal of Dental Research* 89 (2010) 219–229.
- [20] J.J. Elsner, D. Egozi, Y. Ullmann, I. Berdichevsky, A. Shefy-Peleg, M. Zilberman, *Burns* 37 (2011) 896–904.
- [21] R. Pandey, A. Mishra, *Applied Biochemistry and Biotechnology* 160 (2010) 1356–1361.
- [22] M. Sharif Moghaddasi, V. Sandeep Kumar, *International Journal of Biological and Medical Research* 2 (2011) 466–471.
- [23] M.D. Boudreau, F.A. Beland, *Journal of Environmental Science and Health Part C: Environmental Carcinogenesis and Ecotoxicology Reviews* 24 (2006) 103–154.
- [24] Y. Ni, K.M. Yates, I.R. Tizard, in: T. Reynolds (Ed.), *Aloes: The genus Aloe*, CRC Press LLC, New York, 2004.
- [25] A. Djerraba, P. Quere, *International Journal of Immunopharmacology* 22 (2000) 365–372.
- [26] A. Atiba, M. Nishimura, S. Kakinuma, T. Hiraoka, M. Goryo, Y. Shimada, H. Ueno, Y. Uzuka, *American Journal of Surgery* 201 (2011) 809–818.
- [27] S. Jettanacheawchankit, S. Sasithanasate, P. Sangvanich, W. Banlunara, P. Thunyakitpisal, *Journal of Pharmaceutical Sciences* 109 (2009) 525–531.
- [28] T. Salomonson, H.M. Jensen, F.H. Larsen, S. Steuernagel, S.B. Engelsen, *Food Hydrocolloids* 23 (2009) 1579–1586.
- [29] American Society for Testing and Materials, *Annual Book of ASTM Standards*, vol. 06.03, American Society for Testing and Materials, West Conshohocken, PA, 2003, pp. 1–5.
- [30] K. Norajit, K.M. Kim, G.H. Ryu, *Journal of Food Engineering* 98 (2010) 377–384.
- [31] S. Roger, D. Talbot, A. Bee, *Journal of Magnetism and Magnetic Materials* 305 (2006) 221–227.
- [32] C.K. Brown, H.D. Friedel, A.R. Barker, L.F. Buhse, S. Keitel, T.L. Cecil, J. Kraemer, J.M. Morris, C. Reppas, M.P. Stickelmeyer, C. Yomota, V.P. Shah, *AAPS PharmSciTech* 12 (2011) 782–794.
- [33] K.I. Draget, G. Skjåk-Bræk, O. Smidsrød, *International Journal of Biological Macromolecules* 21 (1997) 47–55.
- [34] American Society for Testing and Materials, *Annual Book of ASTM Standards*, vol. 06.01, American Society for Testing and Materials, West Conshohocken, PA, 2000, pp. 1–8.
- [35] M.R. Torres, A.P.A. Sousa, E.A.T. Silva Filho, D.F. Melo, J.P.A. Feitosa, R.C.M. de Paula, M.G.S. Lima, *Carbohydrate Research* 342 (2007) 2067–2074.
- [36] A. Shilpa, S.S. Agrawal, A.R. Ray, *Polymer Reviews* 43 (2003) 187–221.
- [37] J. Ma, H. Wang, B. He, J. Chen, *Biomaterials* 22 (2001) 331–336.
- [38] Q. Wang, X. Hu, Y. Du, J.F. Kennedy, *Carbohydrate Polymers* 82 (2010) 842–847.
- [39] K. Mladenovska, O. Cruaud, P. Richommed, E. Belamie, R.S. Raicki, M.-C. Venier-Julienne, E. Popovski, J.P. Benoit, K. Goracinova, *International Journal of Pharmaceutics* 345 (2007) 59–69.
- [40] L. Chun-hui, W. Chang-hai, X. Zhi-liang, W. Yi, *Process Biochemistry* 42 (2007) 961–970.
- [41] A. Femenia, P. García-Pascual, S. Simal, C. Rosselló, *Carbohydrate Polymers* 51 (2003) 397–405.
- [42] J.P. Soares, J.E. Santos, G.O. Chierice, E.T.G. Cavalheiro, *Eclética Química* 29 (2004) 57–63.
- [43] T. Pongjanyakul, A. Priprem, S. Puttipipatkhachorn, *Journal of Controlled Release* 107 (2005) 343–356.
- [44] T. Pongjanyakul, S. Puttipipatkhachorn, *International Journal of Pharmaceutics* 333 (2007) 34–44.
- [45] B. Hansen, G.B.E. Jemec, *Archives of Dermatology* 138 (2002) 909–911.
- [46] L.W. Chan, H.Y. Lee, P.W.S. Heng, *Carbohydrate Polymers* 63 (2006) 176–187.
- [47] P. Sriamornsak, R.A. Kennedy, *International Journal of Pharmaceutics* 358 (2008) 205–213.
- [48] I. Donati, S. Paoletti, in: B.H.A. Rehm (Ed.), *Alginates: Biology and Applications*, Springer-Verlag, New York, 2009, pp. 1–53.